

Critical properties of the reaction – diffusion model $2A \rightarrow 3A$, $2A \rightarrow \emptyset$

Enrico Carlon^{a,*}, Malte Henkel^a and Ulrich Schollwöck^b

^a*Laboratoire de Physique des Matériaux,** Université Henri Poincaré Nancy I,
B. P. 239, F-54506 Vandœuvre-les-Nancy Cedex, France*

^b*Sektion Physik, Ludwig - Maximilians -Universität München, Theresienstr. 37/III, D-80333 München, Germany*

(March 20, 2019)

The steady-state phase diagram of the one-dimensional reaction-diffusion model $2A \rightarrow 3A$, $2A \rightarrow \emptyset$ is studied through the non-hermitian density matrix renormalization group. In the absence of single-particle diffusion the model reduces to the pair-contact process, which has a phase transition in the universality class of directed percolation (DP) and an infinite number of absorbing steady states. When single-particle diffusion is added, the number of absorbing steady states is reduced to two and the model does not show DP critical behavior anymore. Rather, we find that for large values of the diffusion constant d the transition from the active to the inactive state is of first order. On the other hand, for small values of d the transition is continuous and numerical estimates of the critical exponents are consistent with those of the universality class of the branching-annihilating random walks with an *even* number of offsprings, in spite of the absence of a local conservation law.

05.70.Jk, 05.70.Ln, 64.60.Ht, 02.60.Dc

I. INTRODUCTION

Reaction-diffusion systems have attracted considerable interest in the past few years [1,2]. While at sufficiently high spatial dimensions their critical behavior is correctly described by mean field rate equations, at dimensions below the upper critical dimension, where the effect of fluctuations become important this approach is not valid anymore. In this case one has to resort to other methods as, for instance, field theory [3], exact calculations via Bethe ansatz [4], Monte Carlo and cellular automaton simulations (see [2,5] and references therein) or exact diagonalization techniques [6]. Recently other types of approaches have been proposed as the density matrix renormalization group [7] and the standard real-space renormalization group [8].

In this paper we study the critical properties of a one-dimensional reaction-diffusion model where the local dynamics is given by the following rules. Consider a single species of particles (A) on an one-dimensional lattice. Each lattice site can be either occupied by a single particle or be empty. A single particle may hop to an empty neighboring site (diffusion). Two particles on neighboring sites can either annihilate ($2A \rightarrow \emptyset$) or give birth to a new particle ($2A \rightarrow 3A$) in the case that one of the sites next to the couple is empty. The reaction rates for these processes are defined in equations (1,2,3) below.

Recently, Howard and Täuber [9] discussed a generalized version of the above model where n particles may be created through the reaction $2A \rightarrow (n+2)A$, and with an arbitrary number of particles per site. They employed a field-theoretical approach and found that the theory is not renormalizable. They argued, however, that for all n the model should not be in the directed percolation (DP) universality class. Their conjecture is based on the analysis of the associated master equation and on the

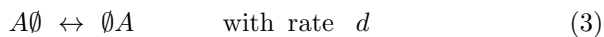
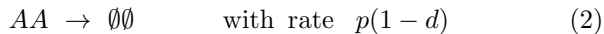
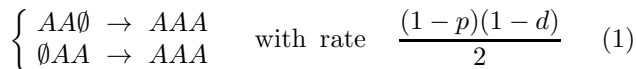
massless nature of the field theory which is at odds with a phase transition of DP type. However, the critical behavior of the system, i.e. its universality class, remained unknown. In absence of diffusion, with at most one particle per site, the $n = 1$ case is the Pair Contact Process (PCP), where the steady-state phase transition belongs to the DP universality class [10].

Here we present a non-perturbative study of the model corresponding to the $n = 1$ case of [9]: the PCP model with additional single-particle diffusion, as obtained from density matrix renormalization group (DMRG) calculations. The DMRG was introduced by White [11] in 1992 to investigate numerically ground state properties of quantum spin chains. Because of its great accuracy, reliability and the possibility of treating large systems with a limited computational effort, the DMRG has since been applied to an ever increasing set of problems, as reviewed in [12]. In particular, some recent studies were devoted to the application of the DMRG to non-hermitian problems [7,13–17] which appear frequently in many domains of physics, for example in low-temperature thermodynamics of spin chains and ladders, for models of the non-integer quantum Hall effect and in one-dimensional non-equilibrium systems. Reaction-diffusion systems belong to the latter class of models. New insight should be expected from the application of the DMRG to them [7].

The paper is organized as follows: in Section II we define the model and recall some facts about reaction-diffusion systems. In Section III we introduce a shift strategy to project out a trivial ground state from the quantum Hamiltonian. This improves the convergence of the DMRG. The method works if an exact expression for the eigenstate is available. In Section IV we discuss the calculation of the critical points and exponents for the model, and show that the model does not belong to the DP universality class. Section V concludes the paper.

II. THE MODEL

We consider a one-dimensional lattice of length L with open boundary conditions, as usual in DMRG calculations [12]. The reactions occur with the following rates



and are parametrized by the diffusion constant d and the pair annihilation rate p .

For a first qualitative overview, we consider the mean field kinetic equations. To discuss the effects of diffusion we need the kinetic equations in the *pair approximation*, see e.g. [2]. If $n = n(t)$ is the spatially averaged single particle density and $c = c(t)$ the spatially averaged pair density, we find

$$\dot{n} = -2(1-d)pc + (1-d)(1-p)(n-c)c/n \quad (4)$$

$$\begin{aligned} \dot{c} = & -(1-d)pc \frac{2c+n}{n} - 2d \frac{(n-c)(c-n^2)}{n(1-n)} \\ & + (1-d)(1-p)(n-c)(1-c)c/(n(1-n)) \end{aligned} \quad (5)$$

In the $d \rightarrow 1$ limit, non-trivial steady states only occur for $c(t) \rightarrow n(t)^2$ and one recovers the single-site kinetic equation (rescaling time by a factor $(1-d)$)

$$\dot{n} = (1-p)n^2(1-n) - 2pn^2 \quad (6)$$

which expresses that particles may only be created on empty sites. The time-dependence of $n(t)$ for t large is

$$n(t) \simeq \begin{cases} n_\infty + \alpha \exp(-t/\tau) & ; \text{ if } p < p_{c,\text{MF}}(1) \\ \sqrt{3/4} \cdot t^{-1/2} & ; \text{ if } p = p_{c,\text{MF}}(1) \\ 1/(3p-1) \cdot t^{-1} & ; \text{ if } p > p_{c,\text{MF}}(1) \end{cases} \quad (7)$$

where $n_\infty = (1-3p)/(1-p)$, $\tau = (1-p)/(1-3p)^2$, $p_{c,\text{MF}}(1) = 1/3$ and α is a constant which depends on the initial conditions. At small p , where the creation process (1) dominates, the system is in the *active* phase with a non-vanishing particle density in the steady state. On the other hand, for p large, the pair annihilation process (2) dominates, the steady state particle density is zero and the system is in the *inactive* phase. In the entire inactive phase, and not only at the critical point, the approach towards the steady state is algebraic, rather than exponential as found in most systems.

The same kind of result also holds in the pair approximation with $d \neq 1$. In the steady state, we have $c(\infty) = n(\infty)(1-3p)/(1-p)$. The particle density vanishes along the curves (i) $p_{c,\text{MF}}(d) = 1/3$ for $1/7 < d \leq 1$ and (ii) $p_{c,\text{MF}}(d) = (1+3d)/(5(1-d))$ for $0 \leq d < 1/7$. Close to the critical curves, $n(\infty) \sim p_{c,\text{MF}}(d) - p$, which is the same found from n_∞ in the $d \rightarrow 1$ limit above.

However, $c(\infty)$ vanishes linearly with $p_{c,\text{MF}}(d) - p$ along the curve (ii) and quadratically along the curve (i). There should thus be different universality classes on both sides of the meeting (“tricritical”) point $p_t = 1/3$ $d_t = 1/7$, where $n(\infty) \sim (p_t - p)^2$ implies modified critical exponents.

Kinetic equations cannot provide correct values of the exponents (and often not even the order of the transition). In one dimension, the exact decay in the inactive phase is $n(t) \sim t^{-1/2}$ [9], where the exponent 1/2 is that of the process $2A \rightarrow \emptyset$ model [18], which is recovered taking the limit $p \rightarrow 1$ in the rates (1) and (2).

An active state with a finite density of particles can be maintained only in the limit $L \rightarrow \infty$. On a finite lattice any configuration of particles will decay towards an absorbing configuration in a finite time. There are two possible absorbing configurations which the system cannot leave: (i) the empty lattice and (ii) a lattice occupied by one single diffusing particle. If we take $d = 0$, we recover the pair contact process (PCP) introduced by Jensen [10]. In that case, any particle configuration without nearest-neighbor pairs is absorbing. The number of absorbing states grows exponentially with the chain length L and it is given by the Fibonacci number (see Appendix A). The steady-state properties of the phase transition between the active and inactive phases are described by the directed percolation (DP) universality class [10]. However, the dynamical properties of this transition are more subtle and still under active investigation [19,20]. As we shall see, the presence of single-particle diffusion changes the universality class of the transition between the active and inactive phases: for any finite values of d it does not fall in the DP universality class anymore.

We find that the transition is of first order for sufficiently large diffusion rates, while it is continuous for small d . In the latter case our numerical estimates of the exponents are consistent with those of the universality class of the branching annihilating random walks (BARW) with an *even* number of offsprings [21]. Long ago, Janssen and Grassberger [22] conjectured that a model with a continuous phase transition from a fluctuating active phase into a phase with a single absorbing state and without additional symmetries is in the DP universality class. While it is widely believed that in the presence of local symmetries in the reaction rates there should be a different universality class (normally the BARW if the particle number is locally conserved modulo 2), Park and Park [23] provided a counterexample which shows that even in the presence of local symmetries the steady-state transition can be in the DP universality class. This already indicates that the universality classification is more subtle than previously thought. The exponents we want to compare with are (see [1,2])

$$\begin{aligned} \text{DP: } & \theta = \nu_{\parallel}/\nu_{\perp} \simeq 1.5806 \dots, \quad \beta/\nu_{\perp} \simeq 0.2520 \dots \\ \text{BARW: } & \theta = \nu_{\parallel}/\nu_{\perp} \simeq 1.749 \dots, \quad \beta/\nu_{\perp} \simeq 0.499 \dots \end{aligned} \quad (8)$$

and are defined as usual from the density $n(p) \sim (p-p_c)^\beta$ and the spatial and temporal correlation lengths $\xi_{\perp, \parallel} \sim (p-p_c)^{-\nu_{\perp, \parallel}}$, see also section IV.

The stochastic time evolution of the system is determined by the master equation, cast into the form

$$\frac{\partial |P(t)\rangle}{\partial t} = -H|P(t)\rangle \quad (9)$$

where $|P(t)\rangle$ a state vector and H is referred to as ‘‘quantum’’ Hamiltonian. For a chain with L sites, H is a stochastic $2^L \times 2^L$ matrix with elements

$$\langle \sigma | H | \tau \rangle = -w(\tau \rightarrow \sigma) \quad , \quad \langle \sigma | H | \sigma \rangle = \sum_{\tau \neq \sigma} w(\sigma \rightarrow \tau)$$

where $|\sigma\rangle, |\tau\rangle$ are the state vectors of the particle configurations σ, τ and w are the transition rates.

Since H is non-hermitian, it has distinct left and right eigenvectors. We will use the notation $|0_r\rangle, |1_r\rangle, \dots, |n_r\rangle$ ($\langle 0_l|, \langle 1_l|, \dots, \langle n_l|$) for the right (left) eigenvectors of H corresponding to energy levels E_0, E_1, \dots, E_n ordered according to $\Re E_0 \leq \Re E_1 \leq \dots \Re E_n$, where \Re denotes the real part. One has $\langle n_l | m_r \rangle = 0$ if $E_n \neq E_m$ and we normalize the states in such a way that $\langle n_l | n_r \rangle = 1$.

Steady states are right eigenvectors of H with zero eigenvalue. The two absorbing configurations mentioned above are steady states and given by

$$|0_r\rangle := |\emptyset \emptyset \emptyset \dots \emptyset\rangle \quad (10)$$

$$|1_r\rangle := |A \emptyset \emptyset \dots \emptyset\rangle + |\emptyset A \emptyset \dots \emptyset\rangle + \dots + |\emptyset \emptyset \emptyset \dots A\rangle \quad (11)$$

Thus, H has two zero eigenvalues $E_0 = E_1 = 0$, while $\Gamma := \Re E_2$ is the inverse relaxation time towards the steady state. Furthermore, since H is stochastic,

$$\langle 0_l | := \sum_{\sigma} \langle \sigma | \quad (12)$$

is a left eigenvector of H with zero eigenvalue.

The calculation of the eigenvalues and eigenvectors of the stochastic Hamiltonian H , from which we will derive the critical properties of the model, is performed by the DMRG algorithm [11,12] adapted to non-hermitian matrices, as described in detail in [7]. In section III we present a further improvement to deal with systems with degenerate ground states.

III. SHIFT OF THE TRIVIAL GROUND STATE

A severe numerical problem is generated by the fact that the physically relevant eigenstate, the first excited state, is only the third state in the spectrum due to the double degeneracy of the ground state. Asymmetric diagonalization algorithms for large sparse matrices are much less robust than their counterparts for symmetric matrices, making a precise determination of eigenvalues not at

the extreme ends of the spectrum much more demanding. In particular, the precision of the eigenstates suffers. This in turn leads to a lower quality truncation of the state space in the DMRG algorithm and subsequently to further deterioration of the results for longer chains. In the present case, the DMRG becomes unstable for rather short chain lengths ($L \approx 20$).

We alleviate this problem successfully by projecting out one of the two ground states, for which both the left and right eigenstate are known, as given in eqs. (12,10). All eigenstates of the asymmetric Hamiltonian H obey a biorthogonality condition, $\langle i_l | j_r \rangle = \delta_{ij}$. This leaves us with two options to eliminate one ground state: (i) Each diagonalization algorithm for large matrices (Arnoldi or Lanczós) generates a sequence of (bi)orthogonal trial vectors, such that the requested eigenstate can be written as a linear combination of those. During the generation, one may enforce orthogonality of all these trial vectors with respect to the ground state. This option does not exist if one uses a black box routine. (ii) One may directly modify the Hamiltonian shifting the ground state to an arbitrarily high energy, i.e. working with:

$$H'(\Delta) := H + \Delta |0_r\rangle \langle 0_l| \quad (13)$$

where Δ is a positive number larger than the energy gap of H . This new Hamiltonian is not stochastic, however it has the same spectrum as H apart from one of the ground states which is shifted to an energy level Δ . The gap can now be obtained from the first excited state of $H'(\Delta)$. This procedure can also be implemented for a stochastic Hamiltonian with a single ground state. The gap is then obtained from the ground state energy of $H'(\Delta)$. This option can always be used independently of the diagonalization method employed.

To implement both options, one has to write down the left and right ground states in the transformed block bases generated by the DMRG .

Let us denote for a block of length L by $|\emptyset_L\rangle$ the state with no particles and by $\langle \tau_L | \equiv \sum_{\sigma_L} \langle \sigma_L |$ the sum over all states of a block (i.e. in the complete, unreduced Hilbert space of the block). In the reduced block basis $\{|m_L\rangle\}$ produced by the DMRG we have approximately $|\emptyset_L\rangle = \sum_{m_L} \langle m_L | \emptyset_L \rangle |m_L\rangle$ and $\langle \tau_L | = \sum_{m_L} \langle \tau_L | m_L \rangle \langle m_L |$. The right and left ground eigenstates then read

$$|0_r\rangle_{2L+2} = |\emptyset_L\rangle \otimes |\emptyset\rangle \otimes |\emptyset\rangle \otimes |\emptyset_L\rangle = \sum_{m_L, m'_L} \langle m_L | \emptyset_L \rangle \langle m'_L | \emptyset_L \rangle (|m_L\rangle \otimes |\emptyset\rangle \otimes |\emptyset\rangle \otimes |m'_L\rangle), \quad (14)$$

$$\langle 0_l |_{2L+2} = \sum_{s, s'} \langle \tau_L | \otimes \langle s | \otimes \langle s' | \otimes \langle \tau_L | = \sum_{m_L, m'_L, s, s'} \langle \tau_L | m_L \rangle \langle \tau_L | m'_L \rangle (\langle m_L | \otimes \langle s | \otimes \langle s' | \otimes \langle m'_L |), \quad (15)$$

where s and s' run over single site states.

At the beginning of the DMRG application, the matrix elements $\langle m_L | \emptyset_L \rangle$ and $\langle \tau_L | m_L \rangle$ are trivially constructed for a sufficiently small L such that the Hilbert space has less than m states, the number of states kept.

Using $\langle \tau_{L+1} | = \sum_s \langle \tau_L | \otimes \langle s |$ and $|\emptyset_{L+1}\rangle = |\emptyset_L\rangle \otimes |\emptyset\rangle$ and inserting one in $\langle \tau_{L+1} | = \sum_{m_{L+1}} \langle \tau_{L+1} | m_{L+1} \rangle \langle m_{L+1} |$ and $|\emptyset_{L+1}\rangle = \sum_{m_{L+1}} \langle m_{L+1} | \emptyset_{L+1} \rangle |m_{L+1}\rangle$ one finds as recursive relation

$$\langle m_{L+1} | \emptyset_{L+1} \rangle = \sum_{m_L} \langle m_{L+1} | m_L \emptyset \rangle \langle m_L | \emptyset_L \rangle, \quad (16)$$

$$\langle \tau_{L+1} | m_{L+1} \rangle = \sum_{m_L, s} \langle m_L s | m_{L+1} \rangle \langle \tau_L | m_L \rangle. \quad (17)$$

The matrix elements $\langle m_{L+1} | m_L s \rangle$ are from the incomplete basis transformation $|m_L\rangle \otimes |s\rangle \rightarrow |m_{L+1}\rangle$.

Numerical implementation of both approaches reveals that the second approach is numerically very stable, while the first one is not, at least not if one carries out an unsophisticated Gram-Schmidt orthogonalization. We suppose that this is due to the fact that global orthogonality of the trial vectors is numerically not exactly conserved by the diagonalization algorithms, while Gram-Schmidt assumes this when a new trial vector is added and made orthogonal to the ground state. As density matrix we have chosen:

$$\rho = \frac{1}{4} \widehat{\text{tr}} \{ |0_r\rangle \langle 0_r| + |0_l\rangle \langle 0_l| + |2_r\rangle \langle 2_r| + |2_l\rangle \langle 2_l| \} \quad (18)$$

where $\widehat{\text{tr}}$ denotes the partial trace on the states of the left or right side of the chain. It is essential to target also the projected ground state to maintain a good description of the ground state via (14) and (15) after some DMRG steps. Otherwise, the Hamiltonian still contains a small perturbing contribution from the zero-energy ground state, which might destroy the stability of the procedure.

IV. NUMERICAL RESULTS

A. Analysis of the gap

We are interested in the lowest energy gap

$$\Gamma = \Gamma(p, d; L) = E_2 \quad (19)$$

whose finite-size scaling behavior contains the desired information about the critical properties of our model (1,2,3). While in principle the eigenvalues of the (non-symmetric) matrix H may have a non-zero imaginary part, we always found that E_2 is real.

Generically, we expect the following finite-size behavior of Γ

$$\Gamma \sim \begin{cases} \exp(-L/\xi_\perp) & ; \text{ if } p < p_c(d) \\ L^{-\theta} & ; \text{ if } p = p_c(d) \\ L^{-2} & ; \text{ if } p > p_c(d) \end{cases} \quad (20)$$

with $\theta = \nu_\parallel/\nu_\perp$ the so-called anisotropy exponent and ξ_\perp the spatial correlation length. At a continuous transition this diverges as $\xi_\perp \sim |p - p_c(d)|^{-\nu_\perp}$, while in the time direction $\xi_\parallel \sim |p - p_c(d)|^{-\nu_\parallel}$.

The first line in (20) indicates that on a finite lattice, the relaxation towards the absorbing configurations is very slow. Indeed, for $L \rightarrow \infty$ the relaxation time $\tau = \Gamma^{-1}$ becomes infinite and a state with a finite density of particles becomes a steady state of the system. From the third line in (20) we see that in the entire inactive phase the scaling behavior of the energy gap is algebraic, with an exponent equal to 2, as for the pair-annihilation model $2A \rightarrow \emptyset$. Therefore, in addition of the obvious double degeneracy of the ground state, we find that our model is gapless in the large-system limit, $\lim_{L \rightarrow \infty} \Gamma(p, d; L) = 0$, for *all* values of p and d (in most systems the gap is finite in the inactive phase).

The different phases and the critical point can be best identified from the analysis of the quantity

$$Y_L(p, d) := \frac{\ln [\Gamma(p, d; L+1)/\Gamma(p, d; L-1)]}{\ln [(L+1)/(L-1)]} \quad (21)$$

While usually, the critical point is found by looking for intersections of two curves Y_L and $Y_{L'}$ for two different lattice sizes L, L' , it turns out that because of the scaling (20), *the critical point is found from the maximum of Y_L as a function of p for fixed d and L* . A scaling argument justifying this criterion is presented in Appendix B. From (20) one then has for the large- L behavior of $Y_L(p, d)$

$$Y_L(p, d) \simeq \begin{cases} -L/\xi_\perp & ; \text{ if } p < p_c(d) \\ -\theta & ; \text{ if } p = p_c(d) \\ -2 & ; \text{ if } p > p_c(d) \end{cases} \quad (22)$$

Therefore, the location of the maximum value of $Y_L(p, d)$ yields a sequence of estimates $p_c(d; L)$ and the value $Y_L(p_c(d; L), d)$ itself yields a sequence θ_L . These sequences converge to the critical point $p_c(d)$ and the anisotropy exponent θ , respectively.

We are now ready to analyze the critical behavior of our model, which turns out to be different at large and small diffusion constants. We start from the former case. Figure 1 shows a plot of $Y_L(p, d)$ as function of the parameter p and for $d = 0.5$. The curves correspond to systems of different sizes: $L = 9$ (upmost curve) 11, 13, 15 and 17 (lowest curve). Calculations were performed up to chains of length $L = 30$.

In the active phase, which extends from $p = 0$ up to $p \approx 0.25$, $Y_L(p, d)$ scales linearly with L as predicted in (22). For larger p the reaction $2A \rightarrow \emptyset$ dominates and the system is in the inactive phase, for which we should have asymptotically $Y_L(p, d) \simeq -2$. As the system size L is increased, the curves approach the expected value -2 in the whole inactive phase. We calculated this

critical exponent accurately by extrapolating the finite-lattice data, using the BST algorithm [24]. Results of the extrapolations for some values of the parameters d and p are shown in Table I. In all cases the extrapolated exponent is in excellent agreement with the expected value of 2, see eq. (22), and with a convergence similar to the examples studied in [7]. This check also confirms that the numerical values for the energy gap, as obtained from the DMRG calculation, are very accurate.

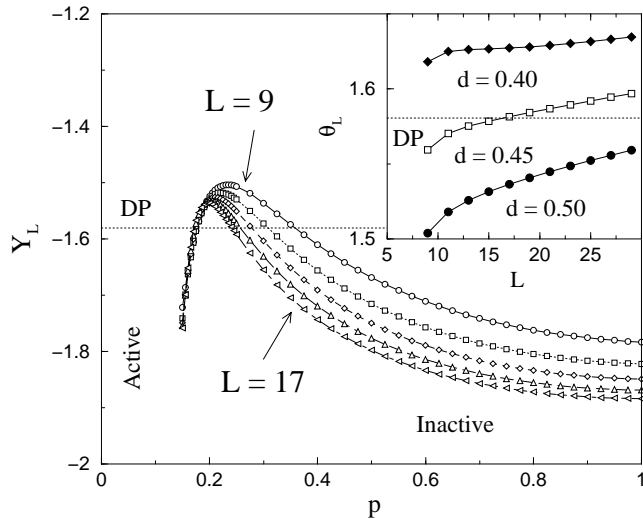


FIG. 1. Plot of $Y_L(p, d)$ as function of p for various lattice sizes ($L = 9, 11, 13, 15, 17$) and $d = 0.5$. The inset shows $\theta_L = \max_p Y_L(p, d = \text{const.})$ as function of the chain length L for $d = 0.4, 0.45$ and 0.5 and L up to 29. The dotted lines labelled DP indicate the value of the anisotropy exponent $\theta_{\text{DP}} = 1.5806\dots$ for directed percolation. If the transition would be in the DP universality class asymptotically we would expect $\theta_L \rightarrow \theta_{\text{DP}}$. The linear scaling of θ_L with L indicates a first-order transition between the active and inactive phases.

TABLE I. Extrapolated exponent $-\lim_{L \rightarrow \infty} Y_L$, obtained by the BST method, of the gap in the inactive phase.

$d = 0.1, p = 0.6$	$d = 0.5, p = 0.6$	$d = 0.8, p = 0.5$
2.0000(1)	2.000(1)	1.99(2)

TABLE II. Critical point estimates $p_c(d)$ as obtained from the energy gap for several values of d .

d	0.10	0.15	0.20	0.40	0.45	0.50
p_c	0.109(2)	0.116(2)	0.121(3)	0.140(1)	0.146(1)	0.152(1)

Next, Table II shows the estimates of the location of the transition point $p_c(d)$ for few values of d . These have been obtained from an $L \rightarrow \infty$ extrapolation of $p_c(L)$, i.e. the abscissas of the maxima of $Y_L(p, d)$. We also recall Jensen's result $p_c(0) = 0.0771$ [10]. All exponent

estimates discussed below are independent of the extrapolated estimates of $p_c(d)$.

We now focus on the properties of the phase transition between the active and inactive phases. For a continuous transition, the sequence θ_L defined above should converge to a finite value, for example to $\theta_{\text{DP}} = 1.5806\dots$, if the transition were in the DP universality class.

The inset of Fig. 1 shows θ_L as a function of the system size L and for $d = 0.50, 0.45$ and 0.40 . In all three cases, and for larger values of the diffusion constant d as well, θ_L does not converge to a finite value as $L \rightarrow \infty$. Rather, it shows a *linear* scaling with L , which is the same scaling behavior as for the active phase, see (22). This means that even at $p = p_c$, the correlation length ξ_{\perp} remains finite. That is evidence for a *first-order* transition, for d sufficiently large.

It is also clear from Fig. 1 that the first-order transition becomes weaker as the diffusion constant is lowered, as the slopes of the lines θ_L vs. L tend to decrease. In particular, this is apparent from the behavior of θ_L for $d = 0.40$. At small system sizes θ_L seems to saturate at a finite value, consistent with a continuous transition, but for $L > 20$ linear scaling sets in. The first-order transition is therefore masked for small L by cross-over effects.

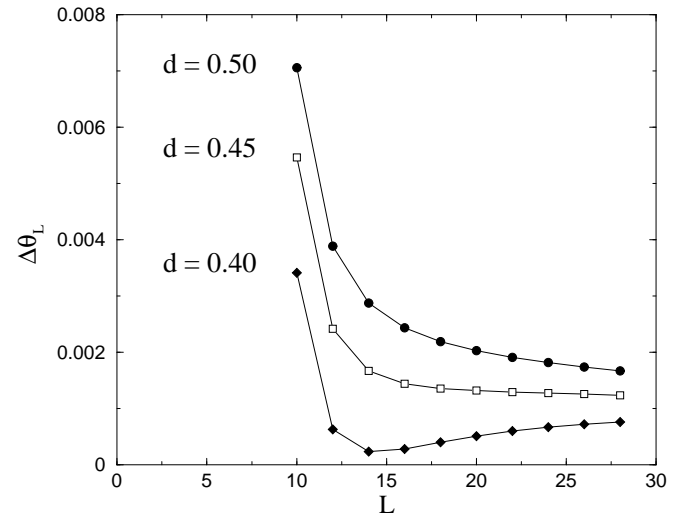


FIG. 2. Numerical derivatives $\Delta\theta_L := \theta_{L+1} - \theta_{L-1}$ as a function of the system size L for several values of d . For $L \rightarrow \infty$, $\Delta\theta_L \rightarrow 2/\xi_{\perp}$, where ξ_{\perp} is the finite correlation length at a first-order transition.

This can be made more explicit by considering the numerical derivative of θ_L , viz. $\Delta\theta_L := \theta_{L+1} - \theta_{L-1}$ as a function of L . In case of a first-order transition, we should have $\theta_L \sim L/\xi_{\perp}$. This implies that $\Delta\theta_L$ should converge to $2/\xi_{\perp}$ as $L \rightarrow \infty$. That is indeed seen in Fig. 2 to be the case and we can estimate $\xi_{\perp} \approx 10^3$ (in units of lattice spacings), which is remarkably large. In spite of this large value of ξ_{\perp} , we stress that the first-order be-

havior is already detectable from our finite lattices with sizes up to $L \approx 30$ (apparently further corrections to scaling are rather weak). For $d = 0.4$, $\Delta\theta_L$ for small L appears to decrease towards zero, as expected for a continuous transition, but for larger L the cross-over towards a first-order transition can be observed.

The scaling behavior of the energy gap for lower values of the diffusion constant is quite different and indicates, instead, a *continuous* transition between the active and the inactive phases. Figure 3 shows a plot of $Y_L(p, d)$ as function of the parameter p , for $d = 0.2$ and $L = 9$ (lowest), 11, 13, 15 and 17 (uppermost). Note that by increasing the system size the maxima shift upwards in Fig. 3, while they shift downwards in Fig. 1. In the inset θ_L as function of $1/L$ is shown for $d = 0.10, 0.15$ and 0.20 . All data converge towards a finite value indicating that the transition is a continuous one.

The values of θ_L as well as the extrapolated estimates for θ , obtained for three values of d , are collected in Table III. In estimating the $L \rightarrow \infty$ limit, we used both the BST algorithm and a simple linear fit in $1/L$, since the data appear to scale nicely with $1/L$, see the inset in figure 3. The exponent θ seems to be weakly dependent on the value of the diffusion constant d , which is probably due to some finite-size corrections. Although BST extrapolations converge well and therefore error bars are small we believe that the method provides values of θ which are somewhat overestimated. Probably this is due to the fact that the accuracy of the original sequence θ_L is not high enough for the BST method to work as efficiently as in other cases [7]. Therefore we keep as final estimates of θ those obtained from the linear fit.

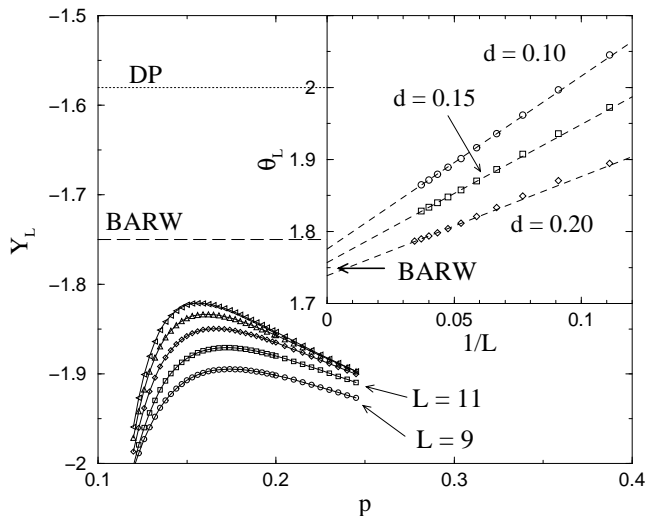


FIG. 3. As in Fig. 1 for $d = 0.2$. The dotted and the dashed-dotted lines indicate the value of the exponent θ for the DP and for the BARW universality class. The inset displays θ_L as function of $1/L$ for three different values of the diffusion constant together with linear fits. The arrow points to $\theta = 1.7499$, see (8).

Comparing these with the values of θ listed in (8), we see that the extrapolated estimates for θ are consistent (except for a slight deviation for the case $d = 0.10$) with the universality class of the BARW with an even number of offsprings. Results are clearly not consistent with a transition of DP type.

TABLE III. Finite-lattice estimates θ_L of the anisotropy exponent for some values of the diffusion constant d . The line labelled BST shows the $L \rightarrow \infty$ values obtained from BST extrapolation and the line labelled LIN those from a linear fit in $1/L$.

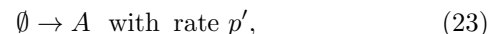
L	$d = 0.10$	$d = 0.15$	$d = 0.20$
9	2.04514424	1.97229158	1.89463046
11	1.99698625	1.93585787	1.87068669
13	1.96187239	1.90730633	1.84951269
15	1.93605523	1.88605871	1.83333869
17	1.91653919	1.87000520	1.82106200
19	1.90138380	1.85759566	1.81161037
21	1.88934458	1.84780200	1.80420811
23	1.87960099	1.83993877	1.79833035
25	1.87159484	1.83353573	1.79361041
27	1.86493230	1.82826331	1.78978671
29			1.78666910
BST	1.813(2)	1.792(2)	1.769(2)
LIN	1.77(1)	1.76(1)	1.74(1)

Between the continuous and the first-order transitions, there should be a “tricritical” point (with different critical exponents), in analogy with the simplest scenario in equilibrium phase diagrams. The properties of the region where first-order and second-order lines meet have not been investigated presently, since this would require a further huge computational effort.

B. Steady state particle density

For a finite lattice and for all values of p and d the stationary states, given in (10) and (11), contain either no or one particle. Therefore the steady-state particle-density vanishes in the large L limit.

To obtain a steady state with a finite density of particles we added a particle creation process at the two boundary sites [7]



We are interested in the (steady state) density profile, for a chain of length L

$$n_L(l) = \langle 0_l | \hat{n}(l) | 0_r \rangle \quad (24)$$

where $l = 1, 2, \dots, L$ labels the position along the chain, $\hat{n}(l)$ is the particle number operator at site l and $|0_r\rangle$

and $\langle 0_i |$ are the left and right ground states of the non-symmetric operator H , with the terms coming from (23) added.

The boundary reaction term removes the ground state degeneracy of H encountered earlier. Therefore, DMRG calculations are easier to perform when $p' \neq 0$. In this case it is not necessary to follow the shift strategy introduced in Sec. III. In fact the DMRG calculations are stable up to chains of lengths $L \approx 50 - 60$, i.e. almost of the double size with respect of the lengths we could reach in the study of the energy gap.

In general, the time-dependent particle density $n = n(t, p; l, L)$ at site l for a lattice of size L and in the vicinity of the critical point, should satisfy the scaling form

$$n(t, p; l, L) = t^{-\beta/\nu_{\parallel}} F(t/\xi_{\parallel}, L/\xi_{\perp}, l/L) \sim \xi_{\perp}^{-\beta/\nu_{\perp}} G(t/\xi_{\perp}^{\theta}, L/\xi_{\perp}, l/L) \quad (25)$$

where for simplicity the dependence on d and p' is suppressed and F and G are scaling functions. The exponents have their usual meaning [2]. In particular, the steady-state density profile, at the critical point, should satisfy

$$n_L(l) := n(\infty, p_c; l, L) = L^{-\beta/\nu_{\perp}} f(l/L) \quad (26)$$

with some scaling function $f(z)$.

First, we consider the inactive phase. For our model, the average particle density decays algebraically for large times as $n(t) \sim t^{-1/2}$. From (25), we identify $\beta/\nu_{\parallel} = 1/2$. Thus $\beta/\nu_{\perp} = \theta\beta/\nu_{\parallel} = 1$ since the anisotropy exponent $\theta = \nu_{\parallel}/\nu_{\perp} = 2$ in the inactive phase, see table I.

The scaling (26) is confirmed in Fig. 4, obtained for chains up to $L = 48$, which shows the scaled particle density $Ln_L(l)$ as a function of l/L . The ratio $\beta/\nu_{\perp} = 1$ for the whole inactive phase has also been confirmed with good accuracy from BST extrapolations.

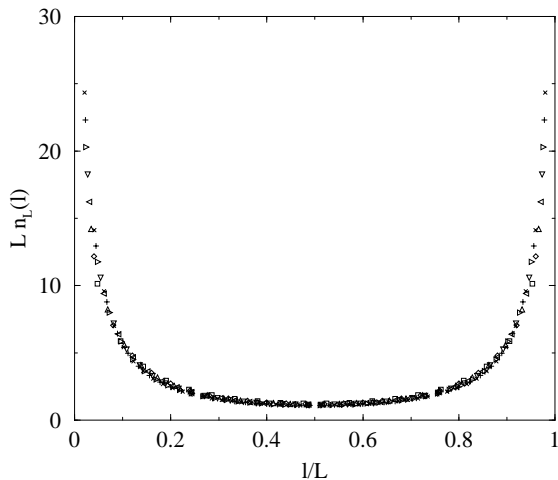


FIG. 4. Scaled particle density $Ln_L(l)$ as function of the scaled variable l/L in the inactive phase for $d = 0.5$, $p = 0.8$ and injection rate $p' = 0.3$. Data for different system sizes ($L = 20, 24, 28, \dots, 48$) collapse nicely onto a single curve.

From now on we focus on the transition between the active and inactive phases. We concentrate on the *central* particle density

$$n(L) := n_L(L/2) \quad (27)$$

For this quantity we expect that for L large, $n(L) \simeq n_0 + O(e^{-L/\xi_{\perp}}) > 0$ in the active phase or at a first-order transition point, where the particle density remains finite. At a continuous phase transition, we expect

$$n(L) \sim L^{-\beta/\nu_{\perp}} \quad (28)$$

In our model, $n(L) \sim L^{-1}$ in the entire inactive phase.

The critical point may be found by adapting the procedure used for the gap Γ . Let $\Delta n(L) := n(L+1) - n(L-1)$ and we have

$$\Delta n(L) \sim \begin{cases} \exp(-L/\xi_{\perp}) & ; \text{ if } p < p_c(d) \\ L^{-1-\beta/\nu_{\perp}} & ; \text{ if } p = p_c(d) \\ L^{-2} & ; \text{ if } p > p_c(d) \end{cases} \quad (29)$$

in complete analogy with (20). Therefore, replacing in the definition (21) the gap $\Gamma(L)$ by $\Delta n(L)$, estimates $p_c(L)$ for the critical point can be obtained as before by looking for the maximum of the Y_L thus redefined. The extrapolated estimates for $p_c(d)$ are shown in Table IV. The results are consistent with the values of p_c obtained from the gap (see Table II) although the error bars are larger in the present case.

TABLE IV. Critical point estimates $p_c(d)$ as obtained from the particle density.

d	0.10	0.15	0.20
p_c	0.114(4)	0.118(3)	0.123(4)

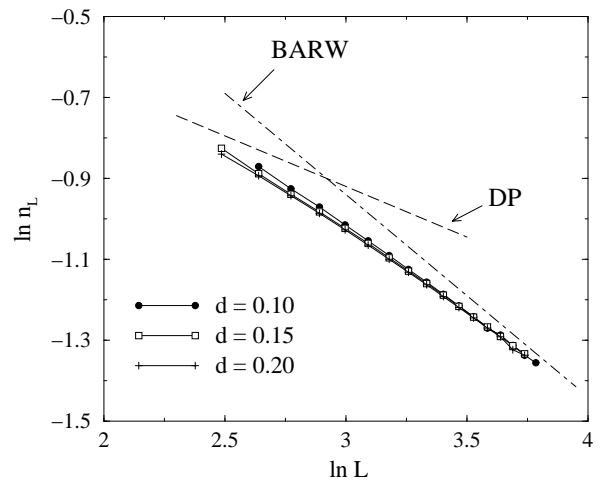


FIG. 5. Central particle density as a function of L at the transition point for several values of d and with boundary injection rate $p' = 0.5$. The slopes of the dashed and dashed-dotted lines correspond to the values of β/ν_{\perp} for the DP and for the BARW universality classes, respectively.

Figure 5 shows a log-log plot of the central particle density $n(L)$ calculated at the finite-size estimate $\bar{p}_c(L)$ of the critical point as a function of the chain length L . The data correspond to $p' = 0.5$ and $d = 0.10, 0.15$ and 0.20 , for which the analysis of the gap indicated a continuous transition.

According to (28) the asymptotic slopes of the curves in Fig. 5 provides an estimate of β/ν_{\perp} . In the figure we have also plotted two straight lines with slopes corresponding to values of β/ν_{\perp} for the DP (dashed line) and for the BARW (dashed-dotted) universality classes, as taken from (8). We see that for L relatively small, the slopes are close to those of directed percolation, before crossing over to some other value (apparently close to the BARW value) as L increases. Clearly, our results are not compatible with the DP universality class. In non-hermitian DMRG the accuracy obtained for the eigenvectors is typically lower than that of the eigenvalues (see discussion in [7]) therefore the precision obtained in the calculation of the particle density is inferior to that of the energy gap. Because of this limited numerical accuracy we did not use the BST method (which requires finite-lattice data with at least 6-7 digits of precision). We used instead a sequence of iterated fits: We first performed a linear fit of groups of four data points in the Fig. 5 from small to large system sizes; the estimated slopes are then extrapolated towards the limit $L \rightarrow \infty$. Results are shown in Table V and are consistent with the BARW universality class.

TABLE V. Extrapolated estimates of the critical exponent β/ν_{\perp} for several values of d .

$d = 0.10$	$d = 0.15$	$d = 0.20$
0.475(20)	0.485(10)	0.490(10)

V. DISCUSSION

Figure 6 shows the phase diagram as found by DMRG calculations. The line marks the locus of phase transition points separating the active from the inactive phase. At $d = 0$ we have indicated the critical point of the PCP model ($p_c(0) = 0.0771$) calculated by Jensen [10], who found that the steady state critical behavior is that of DP. For $d \rightarrow 1$ the transition line seems to terminate in the point $p = 1/3$, which is the same as found from the kinetic equation (7).

Our results indicate that the transition between the active and inactive phases is of first-order type for large diffusion rates and continuous for small diffusion rates. The two regimes are indicated in Fig. 6 by a dashed and by a solid lines respectively. By analogy to equilibrium statistical mechanics, there might be a “tricritical” point at the end of the continuous transition but we point out that this is merely the simplest scenario (in mean-field theory, we also find two distinct transitions in different universality classes which meet in a ‘special’ point, see section II). For the time being, all what we can say is that this point (if it exists) should occur between $d \simeq 0.2$ and $d \simeq 0.4$, since for these cases the transition is continuous or of first order, respectively. Here, we rather focus on the properties of the transition line in the first-order and in the continuous sections.

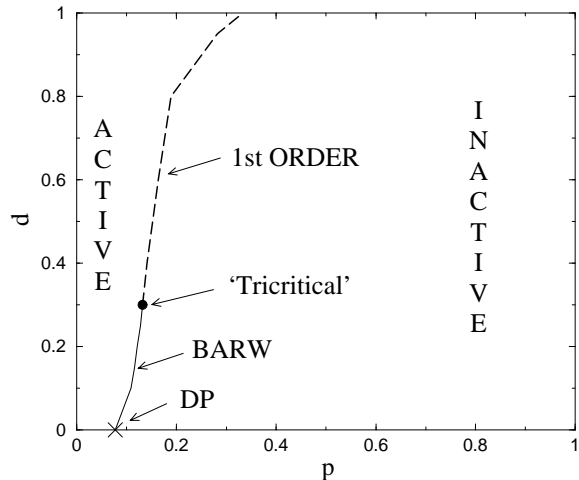


FIG. 6. Phase diagram of the model $2A \rightarrow 3A, 2A \rightarrow \emptyset$ as determined by DMRG techniques. The line separates the active from the inactive phase. The dashed part indicates the locus of first-order transition points. The location of the possible tricritical point is just indicative.

A. The first-order transition

There are several non-equilibrium systems with a first-order transition. Examples are the model introduced by Ziff, Gulari and Barshad [25], the cellular automaton of Bidaux, Boccara and Chaté [26] and the “infection” model studied by Oerding *et al.* [27]. All these models are either multicomponent systems, or the first-order transition occur in dimension larger than one.

The only single-component model with a first-order transition in one dimension we are aware of is the Triplet Creation Model (TCM) studied by Dickman and Tomé [28], defined by the reactions $A \rightarrow \emptyset, 3A \rightarrow 4A$ and diffusion. For sufficiently high diffusion rates the TCM has a first-order transition from an active state into an unique absorbing configuration; the transition becomes contin-

uous and of DP type for lower diffusion rates [28]. The TCM model shows features which resemble those of the phase diagram of Fig. 6 (apart, obviously, from the universality of the continuous transition for which we clearly see non DP behavior). The first-order transition in the TCM seems due to the competition between diffusion and multiparticle creation process. It is also worth stressing that the pair creation model $A \rightarrow \emptyset$, $2A \rightarrow 3A$ has a continuous transition and in the universality class of DP for all values of the diffusion rate. Therefore, it is not easy to see *a priori* from the reaction rates when a model will show a first-order transition or not. Clearly, as pointed out in [28] one needs a mechanism which destabilizes the low density phase. In the present model, this mechanism occurs when diffusion is sufficiently fast, in analogy with [28].

B. The continuous transition

Our numerical calculations yield the final exponent estimates

$$\theta = \nu_{\parallel}/\nu_{\perp} = 1.76(2) \quad , \quad \beta/\nu_{\perp} = 0.48(3) \quad (30)$$

obtained by averaging the results for $d = 0.10$, $d = 0.15$ and $d = 0.20$. The error bars do not contain any systematic error.

These estimates are inconsistent with a transition of DP type (see (8)), a result which is in agreement with the conjecture of [9]. On the other hand, the exponents are consistent with those of the BARW. The BARW universality class is found in different types of models as in some probabilistic cellular automata [29], kinetic Ising models [30] and in transition of systems with two equivalent absorbing states [31].

A prototype of model in the BARW universality class is the reaction-diffusion model $2A \rightarrow \emptyset$, $A \rightarrow (m+1)A$, where m is an even integer. In that model the particles are locally conserved modulo 2. It was commonly believed that local parity conservation was the reason for that model to be in a non-DP universality class. That is not the case, however, as there are models in the BARW universality class with no parity conserving laws. All these models have a common feature: they possess two equivalent absorbing states.

The first step towards a better understanding of the origin of the BARW universality class was made by Park and Park [23] who considered an interacting monomer-dimer model with two equivalent absorbing states and pair-conservation rules. The model falls into the BARW universality class. However, when a parity-conserving field was added, the DP universality class was recovered. If parity conservation *alone* would imply that the system were in the BARW universality class, a parity-conserving field should have no effect on the critical properties of the

model. The parity-conserving field introduced by Park and Park [23] had the effect of favoring one absorbing configuration with respect to the other one. It was concluded [23] that it is the symmetry between absorbing configurations, rather than the pair-conservation rules that is responsible for the system to be in the BARW universality class. These observations were later confirmed by Hinrichsen [31], who studied two different models, both having two equivalent absorbing states, but without parity-conservation laws. Nevertheless, the models were found to belong to the BARW universality class. It was further shown [31] that by introducing a bias in the dynamical rules in such a way that one absorbing configuration is favored with respect to the other the system falls back onto the DP universality class. This brings further evidence that local parity conservation (of the particle number modulo 2) only is neither necessary nor sufficient for a steady-state phase transition to be in the BARW universality class.

The model investigated in this paper does not have *any* parity conservation and has two absorbing configurations given by (10,11). These two are equivalent, in the sense that starting from a random configuration the system evolves towards either one of the two with equal probability. Therefore the situation is similar to the models studied by Hinrichsen [31] and it is not surprising that the transition falls in the same universality class, even in absence of parity conservation.

Finally, we comment on why the numerical estimates for the critical exponents are not as accurate as for DMRG calculations for models in the DP universality class [7]. This is due to the fact that (i) in the present model the ground state is doubly degenerate and the DMRG is known to perform not so well for degenerate spectra (in spite of the improvement introduced in Sec. III) and (ii) the continuous transition seems limited to a narrow interval of values of d . For low d we expect strong finite size effects coming from the fact that the spectrum of H is rather dense near to $E_0 = 0$ (at $d = 0$ the number of ground states grows exponentially with L , see Appendix A) and for larger d , but still in the second-order regime, the vicinity of a higher-order critical point may be responsible for cross-over behavior as well. However, both estimates of $\theta = \nu_{\perp}/\nu_{\parallel}$ and of β/ν_{\perp} are consistent with those of the BARW (in any case, our estimates are of the same degree of precision as other studies which find the BARW universality class in several particle-reaction models, see [2]).

In conclusion, our non-perturbative study of the reactions $2A \rightarrow 3A$ and $2A \rightarrow \emptyset$ with single-particle diffusion has uncovered an unexpectedly complex structure of the phase transition line. Simple symmetry considerations are not enough to predict the universality class of the steady-state phase transition, rather, the precise relationship between the different steady states must be studied. To derive a simple criterion allowing to classify

the critical behavior remains an open challenge.

ACKNOWLEDGMENTS

It is a pleasure to thank M. Howard and U. Täuber for many stimulating discussions and J.F.F. Mendes for participation in the earliest stages of this work. M.H. thanks the Department of Theoretical Physics of the University of Oxford for warm hospitality and J.L. Cardy and Z. Racz for discussions, where early stages of this work were performed. We thank the Centre Charles Hermite in Nancy for providing substantial computational time. E.C. acknowledges a grant from the Ministère des Affaires Étrangères No. 224679A.

APPENDIX A: NUMBER OF ABSORBING CONFIGURATIONS IN THE PCP

For $d = 0$, the model reduces to the pair contact process (PCP) [10]. In this case, all configurations of the type $|\dots \emptyset A \emptyset \dots \emptyset A \emptyset \dots\rangle$, without nearest neighbor particles are absorbing and stationary states. We calculate the number $N(L)$ of absorbing states in the PCP for a chain of length L with free (periodic) boundary conditions.

For *free* boundary conditions, one has the recursion relation

$$N(L) = N(L-1) + N(L-2). \quad (31)$$

To see this, concentrate on the leftmost site. If it is occupied, its neighbor must be empty for the state to be absorbing and there remains an open chain of $L-2$ sites to be considered. If it is empty, one considers the open chain of the remaining $L-1$ sites. The initial conditions for the problem are $N(0) = 1$ and $N(1) = 2$. We see that $N(L) = F_{L+1}$ is the $(L+1)^{\text{th}}$ Fibonacci number.

This can be seen from the generating function

$$\tilde{N}(s) = \sum_{k=0}^{+\infty} N(k) s^k \quad (32)$$

which satisfies because of (31)

$$\tilde{N}(s) = \frac{N(0)(1-s) + N(1)s}{1-s-s^2} = \frac{1+s}{1-s-s^2} \quad (33)$$

For the inverse transformation one can use

$$N(L) = \frac{1}{2\pi i} \oint ds \tilde{N}(s) s^{-L-1} \quad (34)$$

where the integral is taken in a closed circle centered in the origin of the complex s -plane and with radius smaller than the radius of convergence of the series (32), so as to

exclude contributions of other poles than that in $s = 0$. The transformation $z = 1/s$ yields:

$$N(L) = \frac{1}{2\pi i} \oint dz \frac{1+z}{z^2-z-1} z^L = \frac{z_+^{L+2} - z_-^{L+2}}{z_+ - z_-} \quad (35)$$

where $z_{\pm} = (1 \pm \sqrt{5})/2$; z_+ is the golden mean.

For *periodic* boundary conditions, the number $N_{\text{per}}(L)$ of absorbing states for a chain of L sites is

$$N_{\text{per}}(L) = N(L-1) + N(L-3) = z_+^L + z_-^L \quad (36)$$

For L large the asymptotic behavior is $N(L) \sim N_{\text{per}}(L) \sim z_+^L$.

APPENDIX B: FINITE-SIZE-SCALING IN SYSTEMS WITH A CRITICAL PHASE

We discuss the finite-size scaling of the lowest gap $\Gamma = \Gamma_L(p)$ and how to localize the critical point. For simplicity, we suppress the dependence on d and write the scaling form

$$\Gamma_L(p) = L^{-\theta} f\left((p-p_c)L^{1/\nu_{\perp}}\right) \quad (37)$$

where f is assumed to be continuously differentiable. For the gap, one expects the behavior

$$\Gamma_L(p) \sim \begin{cases} e^{-\sigma L} & ; \text{if } p < p_c \\ L^{-2} & ; \text{if } p > p_c, \text{ case C} \\ \Gamma_{\infty} & ; \text{if } p > p_c, \text{ case N} \end{cases} \quad (38)$$

where σ, Γ_{∞} are constants independent of L . Here, case N refers to the “normal” case of non-critical phases on both sides of the transition at $p = p_c$ and case C alludes to the case of a critical phase on one side and we have already set the exponent equal to 2 in view eq. (20) valid for our model. This implies for the scaling function $f(z)$

$$f(z) \sim \begin{cases} \exp(-\text{cste.} |z|^{\nu_{\perp}}) & ; z \rightarrow -\infty \\ z^{(\theta-2)\nu_{\perp}} & ; z \rightarrow +\infty, \text{ case C} \\ z^{\theta\nu_{\perp}} & ; z \rightarrow +\infty, \text{ case N} \end{cases} \quad (39)$$

Since $f(z)$ is positive, it follows that in the case C with $\theta < 2$, $f(z)$ must have a maximum at some finite value z^* . For the case N, however, $f(z)$ should increase monotonically with z .

The estimator Y_L as defined in (21) then becomes

$$Y_L = -\theta + \frac{\ln[f(z_+)/f(z_-)]}{\ln[(L+1)/(L-1)]} \quad (40)$$

where $z_{\pm} = (p-p_c)(L \pm 1)^{1/\nu_{\perp}}$. Furthermore

$$\begin{aligned} \frac{dY_L}{dp} &= \frac{L}{2} \frac{1}{f(z_+)f(z_-)} \\ &\times \left[(L+1)^{1/\nu_{\perp}} f'(z_+)f(z_-) - (L-1)^{1/\nu_{\perp}} f(z_+)f'(z_-) \right] \end{aligned} \quad (41)$$

Now, take the finite-size scaling limit $p \rightarrow p_c$ and $L \rightarrow \infty$ simultaneously such that $z = (p - p_c)L^{1/\nu_\perp}$ is kept fixed. Then both $z_\pm \rightarrow z$ and

$$\lim \frac{dY_L}{dp} \Big|_z = \frac{L^{1/\nu_\perp} f'(z)}{\nu_\perp f(z)} \quad (42)$$

For the case C with $\theta < 2$, we know that there is a z^* such that $f'(z^*) = 0$. If we choose $z = z^*$, we have a sequence of values of p_L converging towards p_c according to $p_L \simeq p_c + z^* L^{-1/\nu_\perp}$. On the other hand, p_L can be found by determining the maximum of Y_L as a function of p , since $\lim dY_L/dp|_{z^*} = 0$ because of (42). This is the desired result. Furthermore, the maximum value $\lim Y_L|_{p=p_L} = -\theta$ because of (40). This allows to find p_c and θ . The generalization to other observables with scaling analogous to (38) is immediate.

For the case N, however, this technique does not apply, since in general $f'(z) > 0$ for all values of z .

* Adress after November, 1st 1999: INFN, Dipartimento di Fisica, Università di Padova, via Marzolo 8, I - 35131 Padova, Italy.

** Unité Mixte de Recherche CNRS No 7556

- [1] V. Privman (Ed.) *Nonequilibrium Statistical Mechanics in One Dimension*, Cambridge University Press (Cambridge 1996)
- [2] J. Marro and R. Dickman, *Nonequilibrium Phase Transitions in Lattice Models* Cambridge University Press (Cambridge 1999)
- [3] J. Cardy and U. C. Täuber, Phys. Rev. Lett. **77**, 4780 (1996) and J. Stat. Phys **90**, 1 (1998); D.C. Mattis and M.L. Glasser, Rev. Mod. Phys. **70**, 979 (1998)
- [4] D. Kandel, E. Domany and B. Nienhuis, J. Phys. A: Math. Gen. **23**, L755 (1990); F.C. Alcaraz, M. Droz, M. Henkel and V. Rittenberg, Ann. of Phys. **230**, 250 (1994); I. Peschel, U. Schultze and V. Rittenberg, Nucl. Phys. **B430**, 633 (1995); P.-A. Bares and M. Mobilia, Phys. Rev. Lett. in press, preprint cond-mat/9909226; G.M. Schütz, *Integrable Stochastic Many-Body Systems*, to appear in C. Domb and J.L. Lebowitz (Eds.), *Phase Transitions and Critical Phenomena* (1999).
- [5] B. Chopard and M. Droz, *Cellular Automata Modelling of Physical Systems*, Cambridge University Press (Cambridge 1998)
- [6] M. Henkel and H. Herrmann, J. Phys. A: Math. Gen. **23**, 3719 (1990); J. de Medonça, Phys. Rev. E **60**, 1329 (1999).
- [7] E. Carlon, M. Henkel and U. Schollwöck, Eur. Phys. J. **B12**, 99 (1999).
- [8] J. Hooyberghs and C. Vanderzande, J. Phys. A: Math. Gen., in press, preprint cond-mat/9903161
- [9] M.J. Howard and U.C. Täuber, J. Phys. A: Math. Gen. **30**, 7721 (1997).
- [10] I. Jensen, Phys. Rev. Lett. **70**, 1465 (1993).
- [11] S.R. White, Phys. Rev. Lett. **69**, 2863 (1992); Phys. Rev. **B 48**, 10345 (1993).
- [12] I. Peschel, X. Wang, M. Kaulke and K. Hallberg (Eds.): *Density Matrix Renormalization: A New Numerical Method in Physics*, Springer, (Heidelberg 1999).
- [13] R.J. Bursill, T. Xiang and G.A. Gehring, J. Phys. Cond. Mat. **8**, L583 (1996); X. Wang and T. Xiang, Phys. Rev. **B56**, 5061 (1997); N. Shibata, J. Phys. Soc. Jpn. **66**, 2221 (1997); K. Maisinger and U. Schollwöck, Phys. Rev. Lett. **81**, 445 (1998).
- [14] Y. Hieida, J. Phys. Soc. Jpn. **67**, 369 (1998).
- [15] M. Kaulke and I. Peschel, Eur. Phys. J. **B5**, 727 (1998).
- [16] Ö. Legeza, M. Kaulke and I. Peschel, Annalen der Physik **8**, 153 (1999)
- [17] J. Kondev and J. B. Marston, Nucl. Phys. **B 497**, 639 (1997); J. B. Marston and Shan-Wen Tsai, Phys. Rev. Lett. **82**, 4906 (1999); T. Senthil, J. B. Marston, and M. P. A Fisher, Phys. Rev. **B 60**, 4245 (1999); Shan-Wen Tsai and J. B. Marston, Annalen der Physik, **8**, Special Issue, 261 (1999).
- [18] L. Peliti, J. Phys. A: Math. Gen. **19**, L365 (1986).
- [19] I. Jensen and R. Dickman, Phys. Rev. E **48**, 1710 (1993); J.F.F. Mendes, R. Dickman, M. Henkel and M.C. Marques, J. Phys. A: Math. Gen. **27**, 3019 (1994); M.A. Munõz, G. Grinstein, R. Dickman and R. Livi, Phys. Rev. Lett. **76**, 451 (1996); P. Grassberger, H. Chaté and G. Rousseau, Phys. Rev. E **55**, 2488 (1997).
- [20] R. Dickman, preprint cond-mat/9909347
- [21] The BARWs with an even and odd number of offsprings are in *distinct* universality classes. In this paper, the BARW universality class *always* refers to the even case.
- [22] H.K. Janssen, Z. Phys. **B42**, 151 (1981); P. Grassberger, Z. Phys. **B47**, 365 (1982)
- [23] H. Park and H. Park, Physica **A221**, 97 (1995)
- [24] R. Burlisch and J. Stoer, Numer. Math. **6**, 413 (1964); M. Henkel and G. Schütz, J. Phys. A: Math. Gen. **21**, 2617 (1988).
- [25] R. Ziff, E. Gulari and Y. Barshad, Phys. Rev. Lett. **56**, 2553 (1986).
- [26] R. Bidaux, N. Boccara and H. Chaté, Phys. Rev. A **39**, 3094 (1989).
- [27] K. Oerding, F. van Wijland, J.-P. Leroy and H.J. Hilhorst, preprint cond-mat/9910351
- [28] R. Dickman and T. Tomé, Phys. Rev. A **44**, 4833 (1991).
- [29] P. Grassberger, F. Krause and T. von der Twer, J. Phys. A: Math. Gen. **17**, L105 (1984); P. Grassberger, J. Phys. A: Math. Gen. **22**, L1103 (1989).
- [30] N. Menyhárd, J. Phys. A: Math. Gen. **27**, 6139 (1994).
- [31] H. Hinrichsen, Phys. Rev. E **55**, 219 (1997)